

High Nuclearity Osmium Cluster Radicalst

Simon R. Drake, Brian F. G. Johnson, Jack Lewis,* and Roderick C. S. McQueen
University Chemical Laboratory, Lensfield Road, Cambridge CB2 1EW

The radical anion species $[\text{Os}_{10}\text{C}(\text{CO})_{24}]^{1-}$ and $[\text{Os}_{10}\text{H}_4(\text{CO})_{24}]^{1-}$ have been prepared by electrochemical and chemical methods ($\text{AgBF}_4\text{-CH}_2\text{Cl}_2$ or $\text{FeCl}_3\text{-tetrahydrofuran}$); as expected they are paramagnetic and exhibit strong signals in their e.s.r. spectra.

The chemical and physical properties of small metallic particles with diameters of less than 100 Å are at present under extensive investigation. This interest arises partly from their situation, *i.e.* intermediate between atomic and metallic regimes,¹⁻³ and also because of their possible catalytic activity.⁴ In contrast to finely-divided metal surfaces, where particle size variation poses major difficulties, high nuclearity metal clusters may be obtained in high purity and are easily structurally characterised by single-crystal X-ray crystallography^{5,6} (see for example Figure 1).

In this paper we report an investigation into the redox chemistry of the two anionic clusters $[\text{Os}_{10}\text{C}(\text{CO})_{24}]^{2-}$ (1) and $[\text{Os}_{10}\text{H}_4(\text{CO})_{24}]^{2-}$ (2) using both electrochemical and chemical methods. By these means the new radical anions $[\text{Os}_{10}\text{C}(\text{CO})_{24}]^{1-}$ (3) and $[\text{Os}_{10}\text{H}_4(\text{CO})_{24}]^{1-}$ (5) have been prepared from their respective dianions (1) and (2).

Results and Discussion

Cyclic voltammetric studies show that in dichloromethane solution at a platinum electrode, salts of the dianionic cluster $[\text{Os}_{10}\text{C}(\text{CO})_{24}]^{2-}$ (1) undergo two oxidation steps (Figure 2). The first is fully reversible ($\Delta E_p = 56$ mV) and corresponds to a simple one-electron oxidation. A plot of i_p vs. $v^{1/2}$ is linear through the origin, and $i_a/i_c = 1$ ($E_3 = +0.78$ V vs. Ag-AgCl). The second is irreversible ($E_p = +1.21$ V vs. Ag-AgCl) and associated with this step is a consequent reduction at +0.35 V vs. Ag-AgCl. Controlled potential electrolysis at +1.0 V in dichloromethane yields a new radical anion $[\text{Os}_{10}\text{C}(\text{CO})_{24}]^{1-}$ (3). This exhibits an i.r. spectrum [$\nu(\text{CO})$ (CH_2Cl_2) at 2054s and 2010s cm^{-1}] similar to that of (1) (2033s and 1988s cm^{-1}), except that all bands are shifted to higher frequency, consistent with the proposed formulation. This species is stable under nitrogen for 2-3 h but on exposure to moist air is quantitatively reduced to the parent dianion (1). Similar behaviour has also been observed in other solvents such as tetrahydrofuran (thf), 1,2-dimethoxyethane, and methyl cyanide. Chemical oxidation of the $[\text{N}(\text{PPh}_3)_2]^+$ salt of (1) with one equivalent of either AgBF_4 in CH_2Cl_2 or FeCl_3 in thf (tetrahydrofuran) produces the same radical anion (Scheme); salts of the new anion (3) could not be separated from the excess of $[\text{N}(\text{PPh}_3)_2]^+$ salts but were characterised on the basis of i.r., mass spectra, electrochemical data, and e.s.r.

Electrogeneration at the potential of the second oxidation (+1.4 V vs. Ag-AgCl) wave at a platinum electrode leads to a new species, $[\text{Os}_{10}\text{C}(\text{CO})_{24}]^{4+}$ (4). This oxidation is irreversible and compound (4) has been isolated as a highly air-sensitive, diamagnetic solid. The same compound is also the product of the chemical oxidation of the $[\text{N}(\text{PPh}_3)_2]^+$ salt of (1) with either AgBF_4 in CH_2Cl_2 or FeCl_3 in thf. It has been characterised on the basis of its spectroscopic and analytical data but it readily reforms (1) upon exposure to moist air.

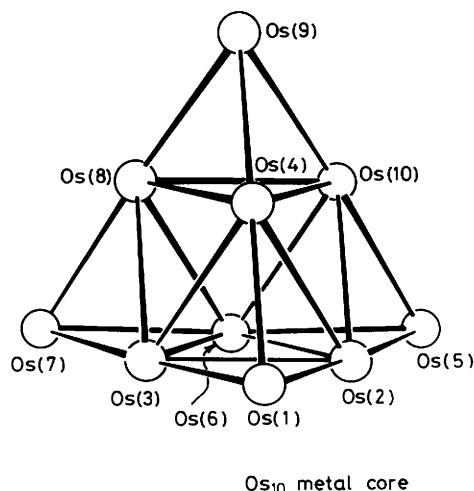


Figure 1. The metal cluster structure on which $[\text{Os}_{10}\text{X}(\text{CO})_{24}]^{2-}$ [$\text{X} = \text{C}$ (1) or H_4 (2)] and its derivatives are based. The carbon atom in (1) occupies an octahedral site, whilst the hydrogen atoms in (2) occupy three tetrahedral sites and the octahedral site

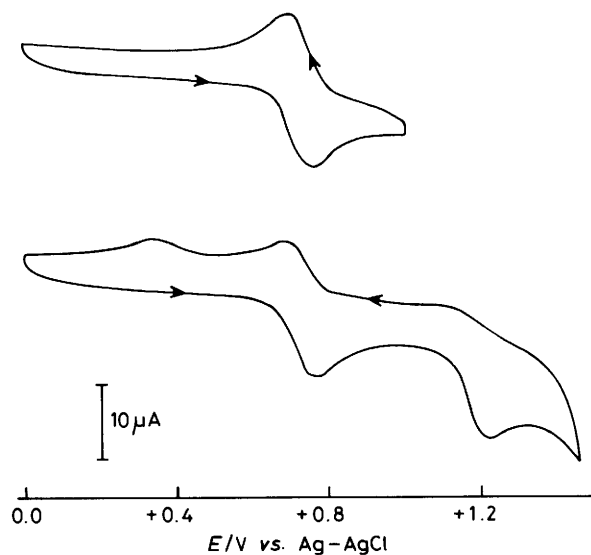
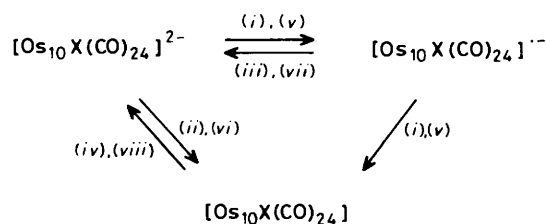


Figure 2. Cyclic voltammogram of 5.5×10^{-6} mol dm^{-3} $[\text{N}(\text{PPh}_3)_2]_2\text{-}[\text{Os}_{10}\text{C}(\text{CO})_{24}]^{2-}$ in 0.2 mol dm^{-3} $\text{NBu}_4\text{BF}_4\text{-CH}_2\text{Cl}_2$ at a platinum electrode. Scan rate 100 mV s^{-1} (at room temperature)

Attempts to obtain a ^{13}C n.m.r. spectrum have, so far, been unsuccessful, since compound (4) is very sparingly soluble in CH_2Cl_2 .

* Non-S.I unit employed: G = 10^{-4} T.



Scheme. X = C: (i) 1 equiv. of AgBF_4 or FeCl_3 , or +1.0 V at a Pt electrode; (ii) 2 equiv. of AgBF_4 or FeCl_3 , or +1.40 V at a Pt electrode; (iii) air for 2–3 min; (iv) acetone, CH_3CN , or heat. X = H₄: (v) 1 equiv. of AgBF_4 or FeCl_3 , or +0.50 V at a Pt electrode; (vi) 2 equiv. of AgBF_4 or FeCl_3 , or +0.70 V at a Pt electrode; (vii) air for up to 12 h; (viii) acetone, CH_3CN , or heat

Similar behaviour has also been observed for the non-carbido cluster $[\text{Os}_{10}\text{H}_4(\text{CO})_{24}]^{2-}$ (2). Cyclic voltammetric studies show that in CH_2Cl_2 solution at a platinum electrode, the $[\text{N}(\text{PPh}_3)_2]^+$ salt of (2) undergoes two oxidation steps. The first corresponds to a fully reversible ($\Delta E_p = 58$ mV) one-electron oxidation with $E_p = +0.39$ V vs. Ag–AgCl. (A plot of i_p vs. $v^{1/2}$ is linear through the origin, and $i_a/i_c = 0.98$.) This value should be compared to the potential (+0.78 V) required to oxidise the corresponding carbido-species (1) to (3). The presence of an electron pair in the highest occupied molecular orbital (h.o.m.o.) of (1) acts as a stabilising influence, with respect to the semi occupied molecular orbital of (3). It was found that (3) was highly air-sensitive since the h.o.m.o. contains one unpaired electron, while the non-carbido radical anion $[\text{Os}_{10}\text{H}_4(\text{CO})_{24}]^{\cdot -}$ (5) is stable in air for up to 12 h.

The second oxidation is irreversible ($E_p = +0.61$ V vs. Ag–AgCl) and associated with this are consequent reductions at +0.13 and –0.27 V vs. Ag–AgCl. Controlled potential electrolysis at +0.50 V vs. Ag–AgCl yields quantitative amounts of $[\text{Os}_{10}\text{H}_4(\text{CO})_{24}]^{\cdot -}$ (5). Chemical oxidation with one equivalent of AgBF_4 in CH_2Cl_2 or FeCl_3 in thf produces the same product which, on prolonged exposure to moist air, reforms the dianion (2). The $[\text{N}(\text{PPh}_3)_2]^+$ salts of both (3) and (5) have been obtained as stable solids (Scheme), under an argon atmosphere. The radical anion (5) could not be obtained in a pure state and has been characterised on the basis of its i.r. and mass spectrum. No hydride signals were observed in the ^1H n.m.r. spectrum of the $[\text{N}(\text{PPh}_3)_2]^+$ salt of (5) in CD_2Cl_2 (see Experimental section).

Electrogeneration of the $[\text{N}(\text{PPh}_3)_2]^+$ salt of (5) at the potential of the second oxidation wave (+0.7 V vs. Ag–AgCl) leads to the formation of a new neutral species $[\text{Os}_{10}\text{H}_4(\text{CO})_{24}]$ (6), which precipitates out of solution as a diamagnetic, brown-black solid. Chemical oxidation of (5) with two equivalents of either AgBF_4 in CH_2Cl_2 or FeCl_3 in thf produces the same product. It is sparingly soluble in CH_2Cl_2 , but is more soluble in a variety of donor solvents such as acetone and reacts with moist air to regenerate the dianion (2) (Scheme).

All clusters (1)–(6) were subjected to fast-atom bombardment (f.a.b.) mass spectroscopy. The highest peak recorded for the clusters (1), (3), and (4) was at $m/z = 2604$ which corresponds to $[\text{Os}_{10}\text{C}(\text{CO})_{24}]^{\cdot -}$ whereas for the clusters (2), (5), and (6) the highest peak occurred at 2596 which corresponds to $[\text{Os}_{10}\text{H}_4(\text{CO})_{24}]^{\cdot -}$ (using ^{192}Os).

As expected, the radical anion species (3) and (5) are paramagnetic. In Figure 3(a) and 3(b) are shown the e.s.r. spectra of these compounds in frozen CH_2Cl_2 solutions at 6 and 9.4 K respectively. For (3) an isotropic value of g of 2.295 is taken as indicative of spin–orbit coupling between various states in the monoanion, while the lineshape⁷ is Lorentzian. The spectrum of a polycrystalline sample of (3) at 7.7 K is nearly

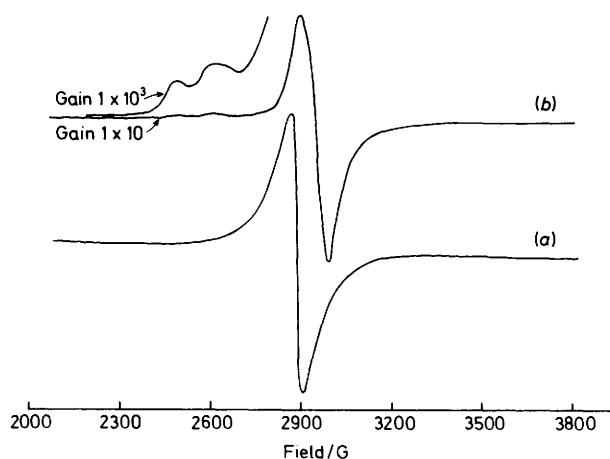


Figure 3. E.s.r. spectra of the radical species $[\text{Os}_{10}\text{C}(\text{CO})_{24}]^{\cdot -}$ (3) (a) and $[\text{Os}_{10}\text{H}_4(\text{CO})_{24}]^{\cdot -}$ (5) (b) recorded at 6 and 9.4 K respectively as frozen CH_2Cl_2 solutions. Modulation 10 G, gain 1×10^1 , ΔH_{pp} (3) = 62 G, ΔH_{pp} (5) = 100 G, and $A/B = 1.0$

identical to that of the frozen solution, being asymmetrical in lineshape and with a value of $g = 2.298$. For (5) the g value of 2.277 is also taken as an indication of spin–orbit coupling. The curve fit is Gaussian, with a large linewidth (100 G at 9.4 K); this is due to unresolved hyperfine coupling from the four hydrogen interstitial atoms. To the left of the main e.s.r. signal for (5) are two weak signals, possibly arising from a certain degree of anisotropy in the radical wavefunction. Previous e.s.r. studies on (1) and $[\text{Os}_{10}\text{H}_2(\text{C})(\text{CO})_{24}]^{\cdot -}$ ⁸ have shown the latter is intrinsically paramagnetic at temperatures below 100 K, giving rise to broad linewidths and values of g close to free spin. With the exception of this species, paramagnetic osmium clusters are rare,^{9,10} and other high nuclearity cluster radicals have also been little studied.^{11,12}

The resonance broadens for these two clusters as the temperature is increased; for (3) a constant linewidth is observed up to 24 K, then as the temperature is raised the linewidth broadens, eventually disappearing above ca. 200 K (the melting point of CH_2Cl_2). For (5) a constant linewidth is observed up to 75 K; above this temperature line broadening occurs and the signal eventually disappears above 200 K.

The relative spin susceptibility has been calculated from the e.s.r. signals for $[\text{Os}_{10}\text{C}(\text{CO})_{24}]^{\cdot -}$ (3) over the temperature range 5–165 K.¹³ The area of the e.s.r. line (assuming a Lorentzian lineshape) is proportional to $(\Delta H_{pp})^2 \times (A + B)$, where ΔH_{pp} is the peak-to-peak linewidth of a first derivative signal, and A and B are the heights of the positive and negative parts of the e.s.r. line. A CuSO_4 standard has been used (one spin per molecule) to determine the number of spins per molecule for (3). Thus (3) was found (by relating the areas under the curves) to have approximately 1 spin per cluster.

The integrated area under the e.s.r. line is a direct measure of the spin susceptibility. Hence, the relative spin susceptibility, $\chi_T/\chi_{77\text{K}} = \chi'(\chi_{77\text{K}}$ taken as standard), can be obtained if the e.s.r. signal area is normalised for both gain and modulation amplitude.

A plot of χ' vs. T gave a Curie-like behaviour. Plotting $1/\chi'$ vs. T gives a straight line, in accord with the Curie law. Since we could not assume total formation of the radical species (3), the value of μ could not realistically be calculated by this method. Instead a room-temperature limiting magnetic moment was obtained from a direct magnetic measurement with the appropriate diamagnetic corrections for the sample container, Os, CO, and $[\text{N}(\text{PPh}_3)_2]\text{Cl}$ being taken into account.¹⁴

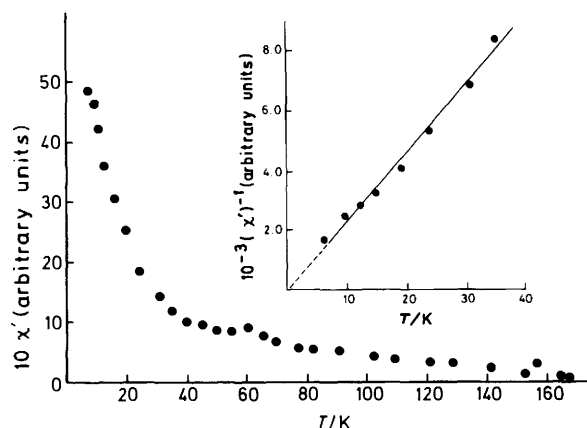


Figure 4. The spin susceptibility of the radical $[\text{Os}_{10}\text{C}(\text{CO})_{24}]^{\bullet-}$ (3) {calculated from e.s.r. data; a plot of χ' vs. temperature is shown, with susceptibility corrected for the diamagnetism of the sample container, Os, CO, and $[\text{N}(\text{PPh}_3)_2\text{Cl}]$. The insert shows a plot of the temperature dependence of the inverse susceptibility for temperatures below 40 K.

A plot of the temperature dependence of the spin susceptibility for (3) is shown in Figure 4 in CH_2Cl_2 . This decanuclear radical exhibits paramagnetism below 293 K in the solid state, conforming exactly with the simple Curie law $\chi_m = C/T$.⁸ The insert in Figure 4 shows a plot of the temperature dependence of the inverse susceptibility for (3) at temperatures below 40 K. A similar temperature dependence is observed for (5), which is in accord with the Curie law. Magnetic moment studies on (3) have shown that this radical species has a magnetic moment of 1.68 ± 0.05 B.M. at 293 K which is in accord with the presence of one unpaired electron. This value (μ) is per cluster {diamagnetic corrections for the sample container, Os, CO, and $[\text{N}(\text{PPh}_3)_2\text{Cl}]$ were also applied}.

The paramagnetic behaviour of these two radical anions contrasts markedly with that of $[\text{Os}_{10}\text{H}_2(\text{C})(\text{CO})_{24}]$ which exhibits intrinsic paramagnetism below 70 K.⁸ A change from Pauli to Curie type behaviour has been predicted,¹⁵ and observed for small metallic particles such as $[\text{Os}_{10}\text{H}_2(\text{C})(\text{CO})_{24}]$, but the precise origins for this behaviour in a *nominally diamagnetic* cluster is still unclear. However, unusual magnetic behaviour has also been observed in small metallic particles;¹⁶ and recently in $[\text{Ni}_{38}\text{Pt}_6(\text{CO})_{48}\text{H}_{6-n}]^{n-}$ ($n = 5$ or 4),¹⁷ where no ¹⁹⁵Pt and ¹H n.m.r. signals were observed, and in other platinum crystallites.¹⁸ On the other hand the two radical species (3) and (5) exhibit paramagnetic behaviour up to 293 K in the solid state, as expected for genuine odd-electron clusters.

Experimental

Infrared spectra were recorded on a Perkin-Elmer PE983 instrument in CH_2Cl_2 at room temperature.

Mass spectra were recorded on a Kratos MS50 mass spectrometer using tris(perfluoroheptyl)-1,3,5-triazine as calibrant and with the instrument in the negative ion fast-atom bombardment mode. The matrix liquid used was glycerol.

Magnetic susceptibility measurements were run on a Johnson Matthey MSB-1 balance at 293 K.

E.s.r. spectra were run on a Varian E109 spectrometer, in the range 4.5–200 K, at a constant magnetic field. Low-temperature work was carried out on an Oxford Instruments e.s.r. 900 Helium Cryostat.

Electrochemical experiments were performed using either a

P.A.R. model 170 or a Metrohm E506/E612 system. Cyclic voltammetry was carried out using a platinum wire electrode (Metrohm EA235) and a platinum wire counter electrode, while the working electrode for controlled potential electrolysis was a gauze basket. The counter electrode was separated from the main cell by a porosity 4 sinter. In CH_2Cl_2 the reference electrode used was Ag–AgCl, whilst in CH_3CN , thf, or 1,2-dimethoxyethane an Ag–AgBF₄ system was used. Maximum care was taken in voltammetry experiments to minimise the effects of solution resistance on the measurements of cathodic and anodic peak potentials. No corrections were made for liquid junction potentials. The use of moderately small electrodes and relatively weak solutions {concentration of $[\text{N}(\text{PPh}_3)_2]_2[\text{Os}_{10}\text{C}(\text{CO})_{24}]$ ca. 5.5×10^{-6} mol dm⁻³} kept currents below 5 μA . All electrode potentials are quoted against the internal marker, ferrocene, whose oxidation occurs at +0.40 V vs. the normal hydrogen electrode. Scan rates were varied within the range 50–500 mV s⁻¹, with 100 mV s⁻¹ as the standard scan rate.

All solvents were distilled prior to use. The supporting electrolyte was NBu_4BF_4 . All electrolyte solutions (0.1 mol dm⁻³ for CH_3CN , thf, or 1,2-dimethoxyethane and 0.2 mol dm⁻³ for CH_2Cl_2) were degassed with argon prior to use and maintained under an argon atmosphere throughout all electrochemical experiments. None of the complexes (3)–(6) may be purified by t.l.c. techniques; the parent dianions (1) and (2) are regenerated. Chemical oxidations were performed under nitrogen using standard Schlenk techniques.

Electrochemical Preparation of $[\text{Os}_{10}\text{C}(\text{CO})_{24}]^{\bullet-}$ (3).—The salt $[\text{N}(\text{PPh}_3)_2]_2[\text{Os}_{10}\text{C}(\text{CO})_{24}]$ (20 mg, 0.0055 mmol) was dissolved in 0.2 mol dm⁻³ NBu_4BF_4 – CH_2Cl_2 (20 cm³). Controlled potential electrolysis at +1.0 V vs. Ag–AgCl yielded the species $[\text{Os}_{10}\text{C}(\text{CO})_{24}]^{\bullet-}$ (3) quantitatively, as judged by i.r. spectroscopy. The radical anion was characterised on the basis of its i.r., e.s.r., and f.a.b. mass spectroscopy. Microanalysis could not be obtained due to the electrolyte being present. I.r.: $\nu(\text{CO})$ at 2 054s and 2 010s cm⁻¹.

Chemical Preparation of $[\text{Os}_{10}\text{C}(\text{CO})_{24}]^{\bullet-}$ (3).—The salt $[\text{N}(\text{PPh}_3)_2]_2[\text{Os}_{10}\text{C}(\text{CO})_{24}]$ (20 mg, 0.0055 mmol) was dissolved in CH_2Cl_2 (10 cm³) and AgBF_4 (1.1 mg, 0.0056 mmol) added. The reaction mixture was left to stir for 1 h, by which time i.r. spectroscopy showed reaction was complete. The solution of (3) was then filtered under N_2 , and slowly reduced in volume to 3 cm³. Hexane (3 cm³) was slowly added to the solution and (3) was isolated in high yield as a brown-black solid. Satisfactory microanalysis could not be obtained for (3) due to the presence of $[\text{N}(\text{PPh}_3)_2]\text{BF}_4$. The radical anion species was characterised by its i.r., f.a.b. mass spectrum, and e.s.r. [This procedure was also used to prepare (3) by oxidation with FeCl_3 in thf.]

Electrochemical Preparation of $[\text{Os}_{10}\text{H}_4(\text{CO})_{24}]^{\bullet-}$ (5).—The salt $[\text{N}(\text{PPh}_3)_2]_2[\text{Os}_{10}\text{H}_4(\text{CO})_{24}]$ (20 mg, 0.0054 mmol) was dissolved in 0.2 mol dm⁻³ NBu_4BF_4 – CH_2Cl_2 (20 cm³). Controlled potential electrolysis at +0.50 V vs. Ag–AgCl yielded $[\text{Os}_{10}\text{H}_4(\text{CO})_{24}]^{\bullet-}$ (5) quantitatively, as judged by i.r. spectroscopy. The radical anion was characterised on the basis of its i.r., f.a.b. mass spectrum, and e.s.r.

The same chemical technique used to oxidise $[\text{N}(\text{PPh}_3)_2]_2[\text{Os}_{10}\text{C}(\text{CO})_{24}]$ to (3) was used to oxidise $[\text{N}(\text{PPh}_3)_2]_2[\text{Os}_{10}\text{H}_4(\text{CO})_{24}]$ to (5) (both CH_2Cl_2 – AgBF_4 and thf– FeCl_3). The radical anion generated was characterised by i.r., f.a.b. mass spectroscopy and ¹H n.m.r. No hydride signals were observed in the ¹H n.m.r. spectrum (400-MHz Brüker instrument; CD_2Cl_2) in the range $\delta +20$ to -50 between 193

* $4\pi \chi_m$ (c.g.s units) = χ_m (S.I.).

and 293 K. I.r.: $\nu(\text{CO})$ at 2 092w, 2 056s, 2 050 (sh), 2 016s (sh), and 2 009s cm^{-1} .

Solutions of (3) and (5) made both chemically and electrochemically were filtered under nitrogen, and freeze-thaw degassed before recording their e.s.r. spectra. Solid samples of (3) and (5) were left under vacuum for 3–4 h before running an e.s.r. spectrum.

Electrochemical Preparation of $[\text{Os}_{10}\text{C}(\text{CO})_{24}]$ (4).—The salt $[\text{N}(\text{PPh}_3)_2]_2[\text{Os}_{10}\text{C}(\text{CO})_{24}]$ (20 mg, 0.0055 mmol) was dissolved in $0.2 \text{ mol dm}^{-3} \text{NBu}_4\text{BF}_4\text{-CH}_2\text{Cl}_2$ (20 cm^3). Controlled potential electrolysis at +1.4 V vs. Ag–AgCl at room temperature yielded species (4) which precipitated out of solution as a black-brown solid. Characterisation of (4) was by i.r. and f.a.b. mass spectroscopy. I.r.: $\nu(\text{CO})$ at 2 078s and 2 034s cm^{-1} .

Chemical Preparation of $[\text{Os}_{10}\text{C}(\text{CO})_{24}]$ (4).—The salt $[\text{N}(\text{PPh}_3)_2]_2[\text{Os}_{10}\text{C}(\text{CO})_{24}]$ (20 mg, 0.0055 mmol) was dissolved in CH_2Cl_2 (10 cm^3) and AgBF_4 (2.2 mg, 0.0112 mmol) added. I.r. spectroscopic monitoring of the solution showed that the reaction was complete after ca. 1 h at room temperature, with precipitation of (4). The species (4) was isolated in near-quantitative yield by filtration as a brown-black solid. Characterisation of (4) was by i.r., f.a.b. mass spectroscopy, and microanalysis (Found: C, 11.40. Calc. for $\text{C}_{25}\text{O}_{24}\text{Os}_{10}$: C, 11.50%). The same technique was used to oxidise the $[\text{N}(\text{PPh}_3)_2]^+$ salt of (1) to (4), using 2 equivalents of FeCl_3 in thf.

Electrochemical Preparation of $[\text{Os}_{10}\text{H}_4(\text{CO})_{24}]$ (6).—The salt $[\text{N}(\text{PPh}_3)_2]_2[\text{Os}_{10}\text{H}_4(\text{CO})_{24}]$ (20 mg, 0.0054 mmol) was dissolved in $0.2 \text{ mol dm}^{-3} \text{NBu}_4\text{BF}_4\text{-CH}_2\text{Cl}_2$ (20 cm^3). Controlled potential electrolysis at +0.70 V vs. Ag–AgCl at room temperature yielded $[\text{Os}_{10}\text{H}_4(\text{CO})_{24}]$ (6) which precipitated out of solution as a brown-black solid. Characterisation of this species was by i.r. and f.a.b. mass spectroscopy. I.r.: $\nu(\text{CO})$ at 2 106w, 2 080s, 2 068s (sh), 2 050m (sh), 2 035s, and 2 014m (sh) cm^{-1} .

Chemical Preparation of $[\text{Os}_{10}\text{H}_4(\text{CO})_{24}]$ (6).—The salt $[\text{N}(\text{PPh}_3)_2]_2[\text{Os}_{10}\text{H}_4(\text{CO})_{24}]$ (20 mg, 0.0054 mmol) was dissolved in CH_2Cl_2 (10 cm^3) and AgBF_4 (2.2 mg, 0.0112 mmol) added. I.r. spectroscopic monitoring of the solution showed that the reaction was complete after ca. 0.5 h at room temperature, with precipitation of $[\text{Os}_{10}\text{H}_4(\text{CO})_{24}]$ (6). The cluster (6) was isolated in near-quantitative yield by filtration as a brown-

black solid. Characterisation of (6) was by i.r., f.a.b. mass spectroscopy, and microanalysis (Found: C, 11.25; H, 0.20. Calc. for $\text{C}_{24}\text{H}_4\text{O}_{24}\text{Os}_{10}$: C, 11.05; H, 0.10%).

The same technique was used to oxidise the $[\text{N}(\text{PPh}_3)_2]^+$ salt of (2) to (6) using 2 equivalents of FeCl_3 in thf.

Acknowledgements

We are grateful to the S.E.R.C. for financial support (to S. R. D.) and also Mr. P. A. Loveday for his invaluable help with the e.s.r.

References

- 1 R. E. Benfield, P. P. Edwards, W. J. H. Nelson, M. D. Vargas, D. C. Johnson, and M. J. Sienko, *Nature (London)*, 1985, 314.
- 2 R. C. Baetzold, *Inorg. Chem.*, 1981, 20, 118.
- 3 M. R. Harrison and P. P. Edwards, 'Metallic and Non-Metallic States of Matter', eds. P. P. Edwards and C. N. R. Rao, Taylor and Francis Ltd., London, 1985, ch. 14.
- 4 F. Hugues, P. Besson, P. Bussiere, J. A. Dalmon, J. M. Basset, and D. Olivier, *Nouv. J. Chim.*, 1981, 5, 207.
- 5 P. F. Jackson, B. F. G. Johnson, J. Lewis, M. McPartlin, W. J. H. Nelson, and M. D. Vargas, *J. Chem. Soc., Chem. Commun.*, 1983, 224.
- 6 D. Braga, J. Lewis, B. F. G. Johnson, M. McPartlin, W. J. H. Nelson, and M. D. Vargas, *J. Chem. Soc., Chem. Commun.*, 1983, 241.
- 7 P. W. Atkins and M. C. R. Symons, 'The Structure of Inorganic Radicals', Elsevier, Amsterdam, 1967.
- 8 R. E. Benfield, P. P. Edwards, and M. M. Stacy, *J. Chem. Soc., Chem. Commun.*, 1982, 525.
- 9 B. M. Peake, B. H. Robinson, J. Simpson, and D. J. Watson, *J. Chem. Soc., Chem. Commun.*, 1974, 945.
- 10 B. M. Peake, B. H. Robinson, J. Simpson, and D. J. Watson, *Inorg. Chem.*, 1980, 19, 465.
- 11 T. Baringhelli, F. Morazzoni, and D. Strumolo, *J. Organomet. Chem.*, 1982, 236, 109.
- 12 G. Longoni and F. Morazzoni, *J. Chem. Soc., Dalton Trans.*, 1981, 1735.
- 13 C. P. Poole, 'Electron Spin Resonance', John Wiley, New York, 1983, ch. 12.
- 14 E. König, 'Landolt-Bornstein', Springer-Verlag, Berlin, 1966, vol. 2.
- 15 H. Fröhlich, *Phys. Scr.*, 1937, 4, 406; R. Kubo, *J. Phys. Soc. Jpn.*, 1982, 17, 975; R. F. Marzke, *Catal. Rev. Sci. Engl.*, 1979, 19, 43.
- 16 J. L. Carter and J. H. Sinfelt, *J. Catal.*, 1968, 10, 134.
- 17 A. Ceriotti, F. Demartin, G. Longoni, M. Manassero, M. Marchionna, G. Piva, and M. Sansoni, *Angew. Chem., Int. Ed. Engl.*, 1985, 24, 697.
- 18 R. F. Marzke, W. S. Glaunsinger, and M. Bayard, *Solid State Commun.*, 1976, 18, 1025.

Received 24th March 1986; Paper 6/580